Electronic Supporting Information for

Insights into the Charge-Transfer Character of Electronic Transitions in $^{R}Cp_2Ti(C_2Fc)_2$ Complexes Using Solvatochromism, Resonance Raman Spectroscopy, and TDDFT

Elizabeth S. Carlton,[a] Joshua J. Sutton,[b] Ariel G. Gale,[a] George C. Shields,[a] Keith C. Gordon,[b] and Paul S. Wagenknecht[a,*]

[a] Department of Chemistry, Furman University, Greenville, SC, 29613 USA
[b] Department of Chemistry, University of Otago, P.O. Box 56, Dunedin, New Zealand

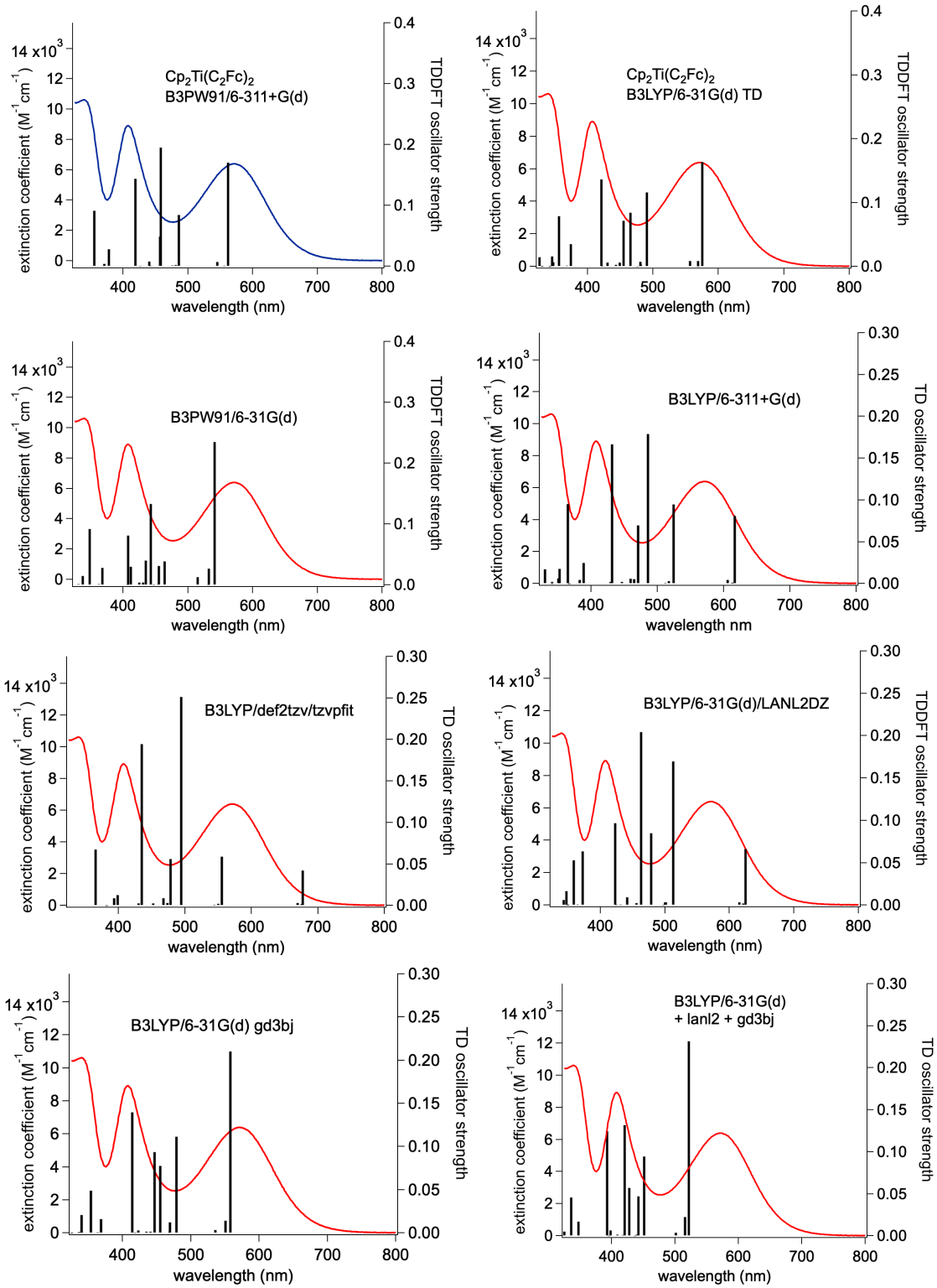

Figure S1. Overlay of experimental spectra and TDDFT predicted vertical transitions and oscillator strengths for various computational models. All computational models utilize solvent=thf. Optimization and TDDFT were performed within the same computational model.

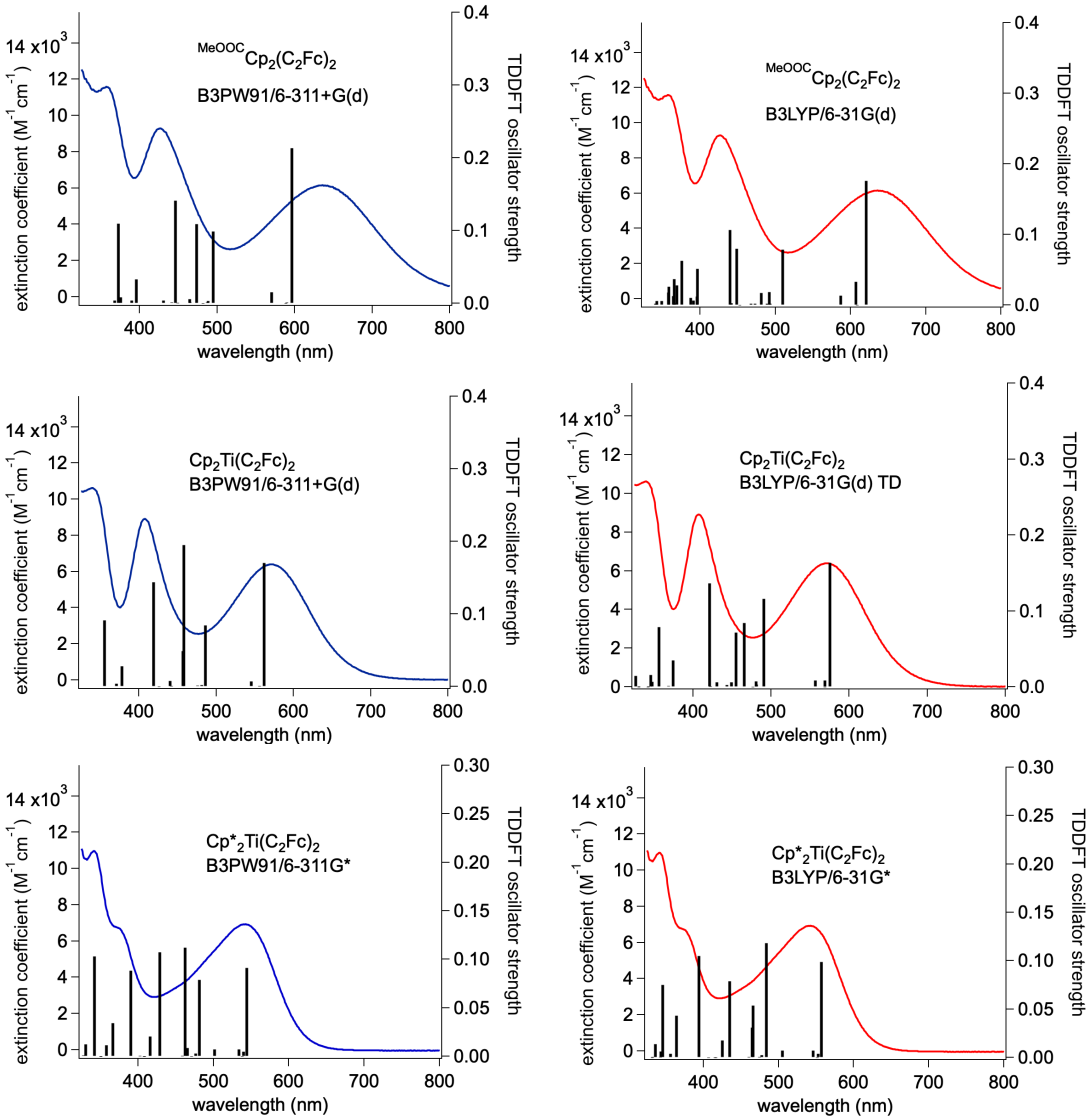

Figure S2. Overlay of experimental spectra and TDDFT predicted vertical transitions and oscillator strengths (B3PW91/6-311+G(d) (left) vs B3LYP/6-31G(d) (right)) for $^{MeOOC}Cp_2Ti(C_2Fc)_2$ (top), $Cp_2Ti(C_2Fc)_2$ (middle), and $Cp^*_2Ti(C_2Fc)_2$ (bottom). Comparison of. The experimental spectra were recorded in THF. Optimization and TDDFT employed a THF solvent model.

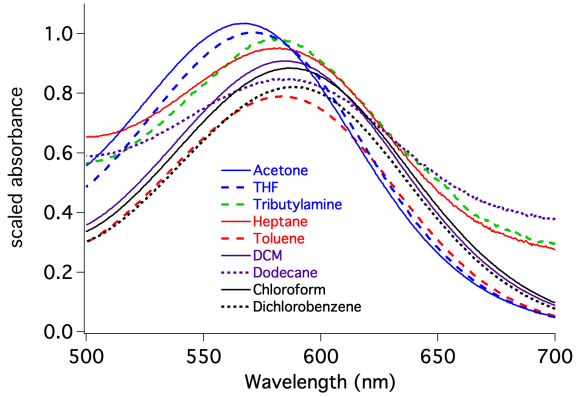

Figure S3. Solvatochromic data for remaining solvents not shown in manuscript Figure 5 for $Cp_2Ti(C_2Fc)_2$. Absorbance is scaled to allow observation of all peaks.

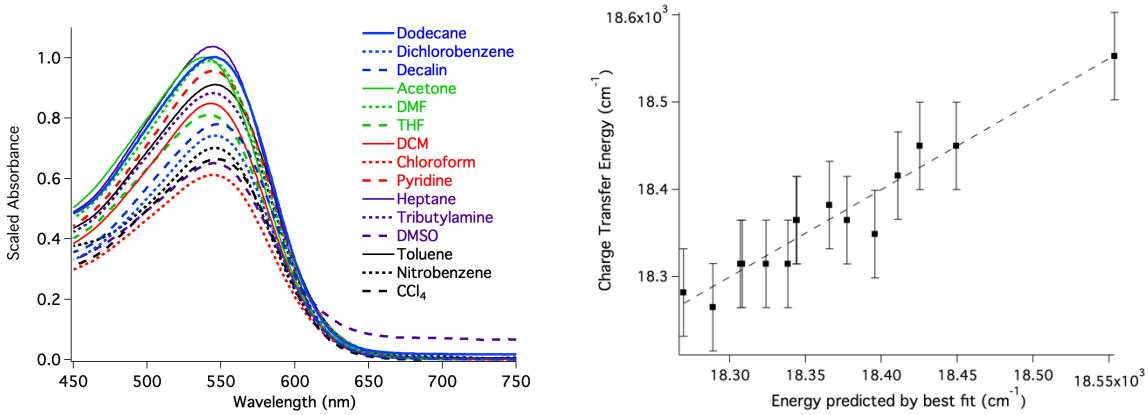

Figure S4. Solvatochromic data (left) for $Cp^*_2Ti(C_2Fc)_2$ along with a representation of the goodness of fit to equation 1 (right). Absorbance is scaled to allow observation of all peaks. Wavelengths recorded in manuscript Table 1.

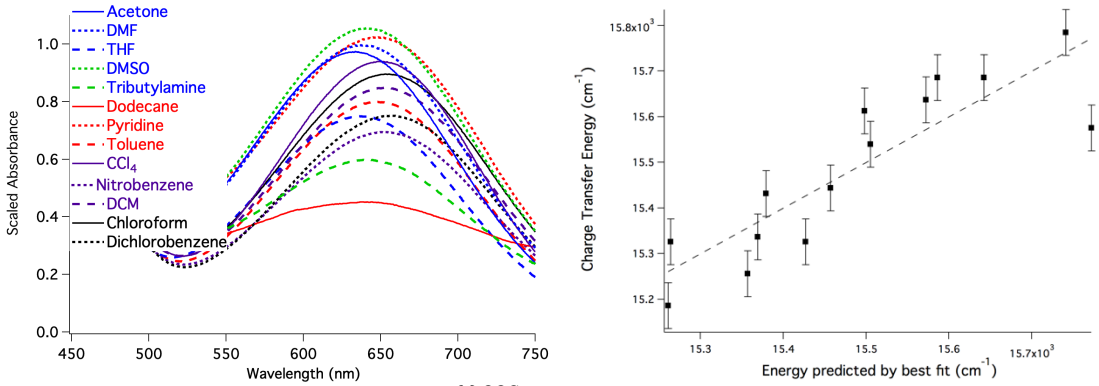

Figure S5. Solvatochromic data (left) for $^{MeOOC}Cp_2Ti(C_2Fc)_2$ along with a representation of the goodness of fit to equation 1 (right). Absorbance is scaled to allow observation of all peaks. Wavelengths recorded in manuscript Table 1.

Table S1. TDDFT output for key excited states for $Cp_2Ti(C_2Fc)_2$

Excited State 1: Singlet-A 2.1531 eV 575.83 nm f=0.1641 <S**2>=0.000

149 ->160	0.11398
150 ->161	-0.15130
151 ->154	-0.10597
151 ->162	-0.15164
152 ->157	0.15329
152 ->159	-0.21372
153 ->154	***0.52541***
153 ->160	0.22823

Excited State 5: Singlet-A 2.5271 eV 490.61 nm f=0.1154 <S**2>=0.000

145 ->154	0.11302
145 ->160	0.14732
146 ->159	-0.11019
148 ->154	-0.14690
149 ->154	-0.20214
150 ->161	***0.32404***
151 ->154	-0.10063
151 ->162	***0.31696***
152 ->159	0.11317
153 ->154	***0.30064***
153 ->160	-0.11676

Excited State 15: Singlet-A 2.9409 eV 421.58 nm f=0.1393 <S**2>=0.000

148 ->154	-0.31042
149 ->154	***0.56369***
150 ->161	0.10714
151 ->162	0.12056

Excited State 18: Singlet-A 3.4794 eV 356.34 nm f=0.0807 <S**2>=0.000

144 ->154	***0.62626***
147 ->154	0.13737
152 ->160	0.10680
153 ->159	-0.10839

Table S2. Orbitals involved in key excited states for $Cp_2Ti(C_2Fc)_2$

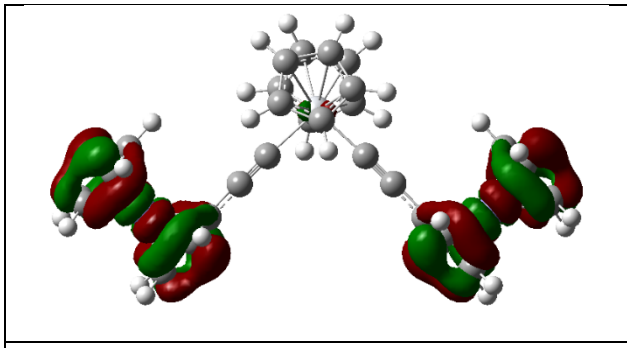	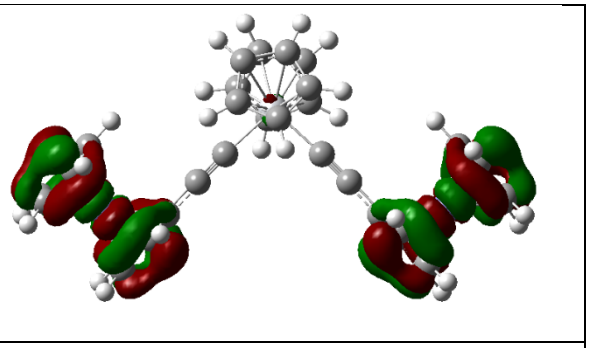
162	161
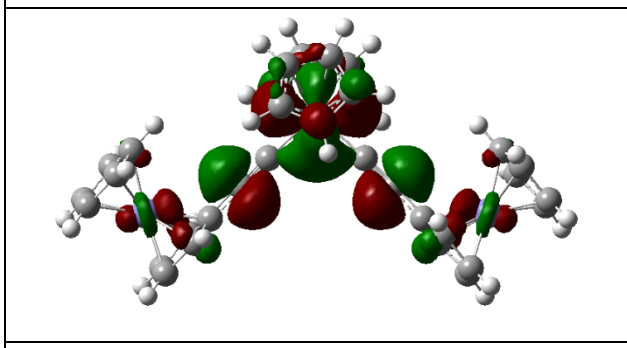	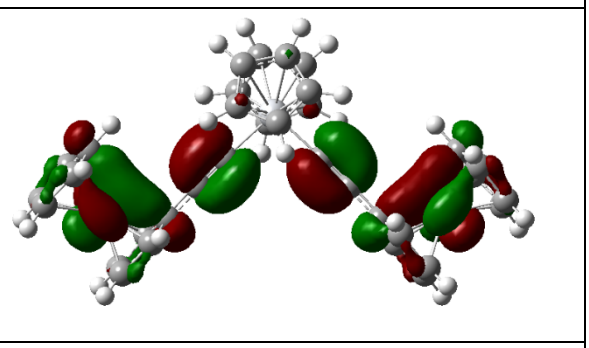
154 LUMO	153 HOMO
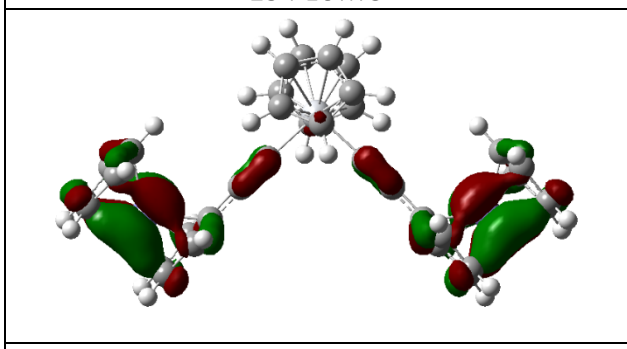	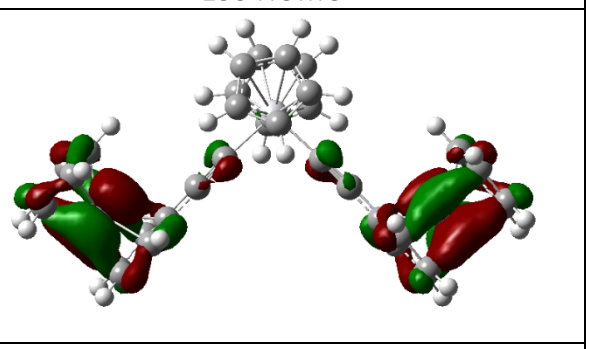
151	150
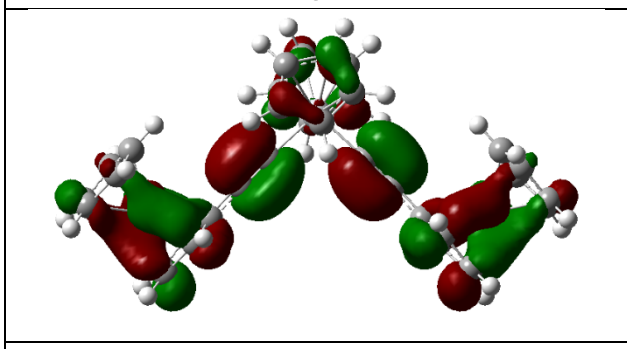	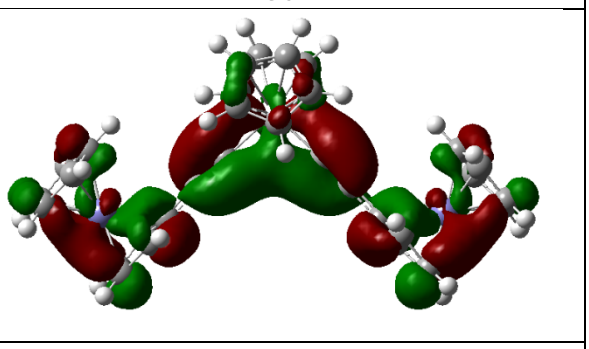
149	144

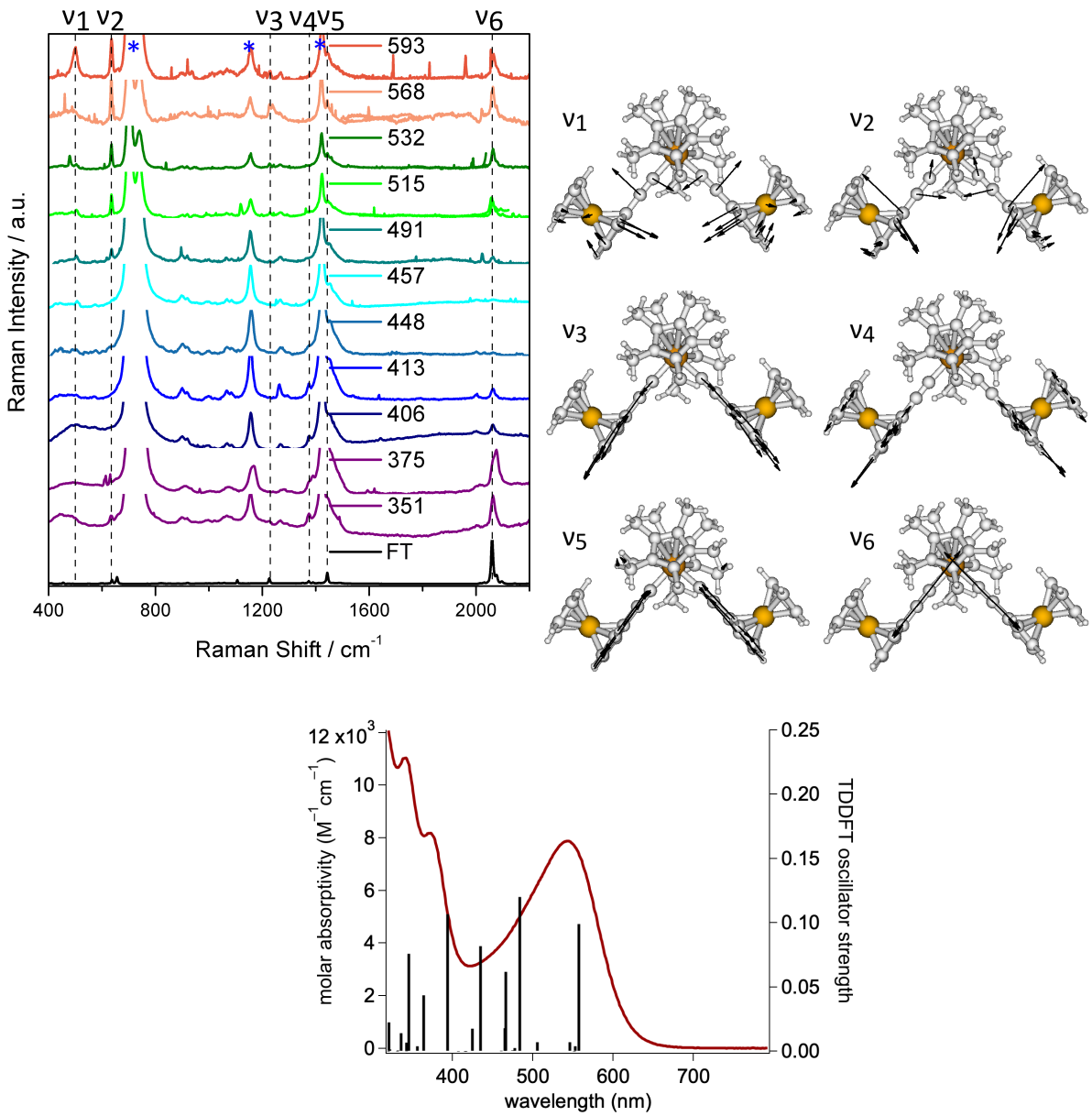

Figure S6. Top Left: Resonance Raman spectra for $Cp^*_2Ti(C_2Fc)_2$ in CH_2Cl_2, at the wavelengths listed (solvent bands are marked with *). Top Right: Key vibrational modes. Bottom: Overlay of experimental UV-Vis in CH_2Cl_2 with TDDFT predicted vertical transitions. Vibrational modes and TDDFT vertical transitions modelled in CH_2Cl_2 using B3LYP/6-31G(d).

Table S3. Key electronic transitions of $Cp^*_2Ti(C_2Fc)_2$ with associated changes in electron density.[a]

λ (nm)	Oscillator Strength	Ti	Cp^*_{Ti}	Fe	C_2Cp_{Fe}	Cp_{Fe}
557	0.099	1→33 (32)	6→8 (2)	58→29 (-29)	27→22 (-5)	8→9 (1)
483	0.120	2→27 (25)	11→6 (-5)	60→36 (-24)	20→21 (1)	7→10 (3)
435	0.082	5→52 (47)	24→9 (-15)	39→12 (-27)	28→24 (-4)	5→3 (-2)
393	0.107	8→54 (46)	40→10 (-30)	18→9 (-9)	29→24 (-5)	4→3 (-1)
345	0.076	5→54 (49)	11→10 (-1)	33→9 (-24)	43→24 (-19)	8→3 (-5)

[a] Calculated from a Mulliken population analysis from the TDDFT data calculated at the B3LYP/6-31G(d) level using solvent = CH_2Cl_2.

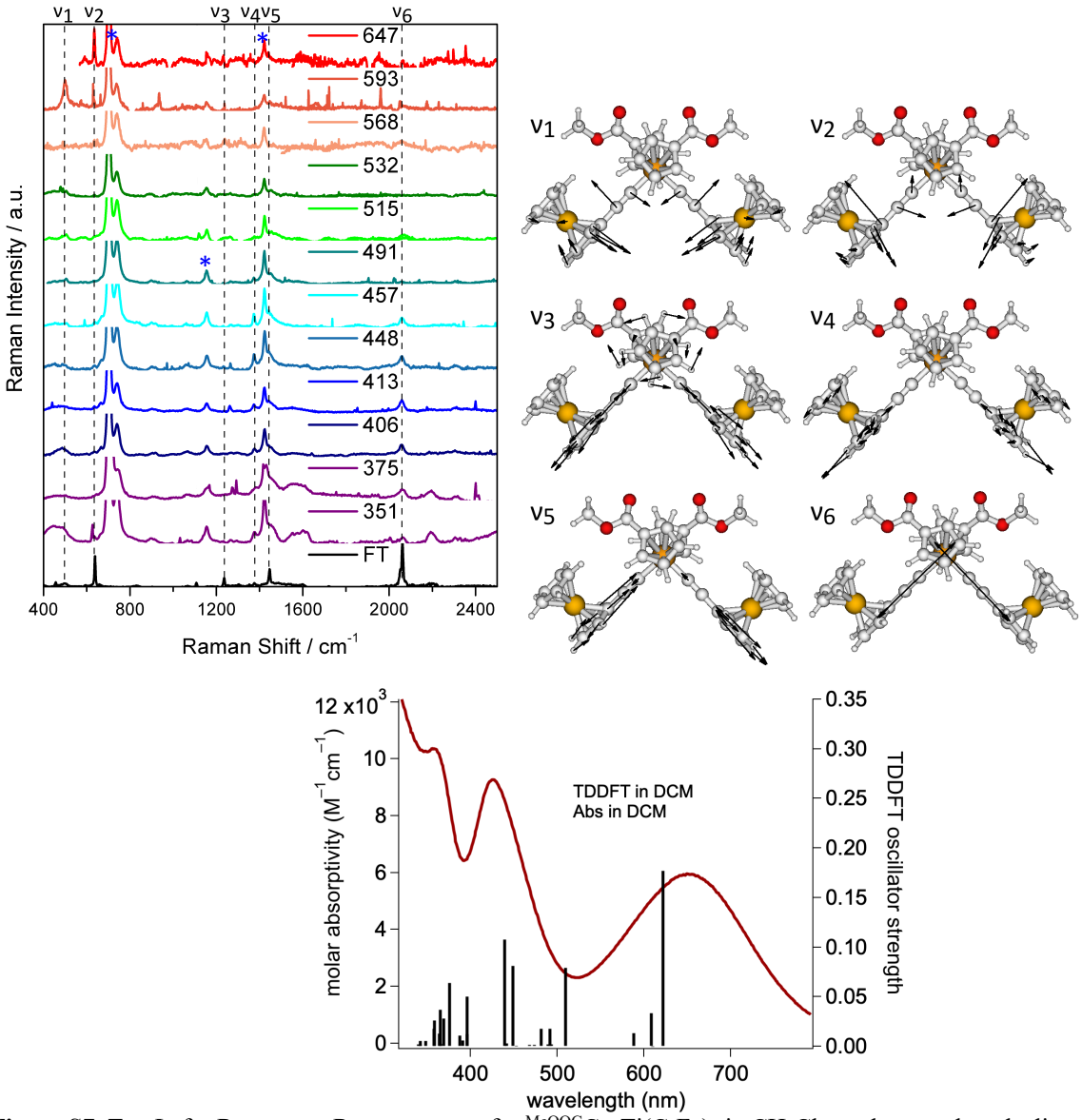

Figure S7. Top Left: Resonance Raman spectra for $^{MeOOC}Cp_2Ti(C_2Fc)_2$ in CH_2Cl_2, at the wavelengths listed (solvent bands are marked with *). Top Right: Key vibrational modes. Bottom: Overlay of experimental UV-Vis in CH_2Cl_2 with TDDFT predicted vertical transitions. Vibrational modes and TDDFT vertical transitions modelled in CH_2Cl_2 using B3LYP/6-31G(d).

Table S4. Key electronic transitions of $^{MeOOC}Cp_2Ti(C_2Fc)_2$ with associated changes in electron density.[a]

λ (nm)	Oscillator Strength	Ti	$^{MeOOC}Cp_{Ti}$	Fe	C_2Cp_{Fe}	Cp_{Fe}
622	0.177	0→53 (53)	2→13 (11)	66→9 (-57)	23→23 (0)	9→2 (-7)
510	0.079	1→32 (31)	5→11 (6)	55→28 (-27)	31→21 (-10)	8→8 (0)
439	0.108	2→45 (43)	16→11 (-5)	42→16 (-26)	36→22 (-14)	4→5 (1)
376	0.063	5→56 (51)	12→17 (5)	18→5 (-13)	55→22 (-33)	9→1 (-8)

[a] Calculated from a Mulliken population analysis from the TDDFT data calculated at the B3LYP/6-31G(d) level using solvent = CH_2Cl_2.

Table S5. TDDFT output for key excited states for $Cp^*_2Ti(C_2Fc)_2$

Excited State 1: Singlet-B 2.2242 eV 557.43 nm f=0.0991 <S**2>=0.000

188 ->199	0.14367
190 ->197	0.10008
190 ->201	0.18408
191 ->197	-0.21223
191 ->200	0.19439
192 ->202	0.18314
193 ->194	***0.43787***
193 ->199	0.25319

Excited State 6: Singlet-B 2.5629 eV 483.77 nm f=0.1201 <S**2>=0.000

183 ->194	-0.14183
183 ->199	-0.19244
184 ->197	0.13123
184 ->200	-0.12561
188 ->194	-0.22344
189 ->202	0.13482
190 ->201	-0.23857
191 ->201	-0.19030
192 ->202	***-0.28147***
193 ->194	***0.34073***

Excited State 12: Singlet-B 2.8500 eV 435.03 nm f=0.0819 <S**2>=0.000

183 ->194	-0.17627
183 ->199	-0.14851
186 ->194	***0.35299***
188 ->194	-0.29949
193 ->194	***-0.34280***
193 ->199	0.16542

Excited State 17: Singlet-B 3.1487 eV 393.76 nm f=0.1069 <S**2>=0.000

186 ->194	***0.52378***
188 ->194	***0.39168***
190 ->201	-0.10880
192 ->202	-0.12284

Excited State 20: Singlet-A 3.5858 eV 345.77 nm f=0.0758 <S**2>=0.000

181 ->194	-0.14808
182 ->194	***0.54852***
184 ->194	-0.13901
185 ->194	-0.14871
190 ->199	-0.10657
192 ->201	-0.10050
193 ->197	-0.11328

Table S6. Orbitals involved in key excited states for $Cp^*_2Ti(C_2Fc)_2$

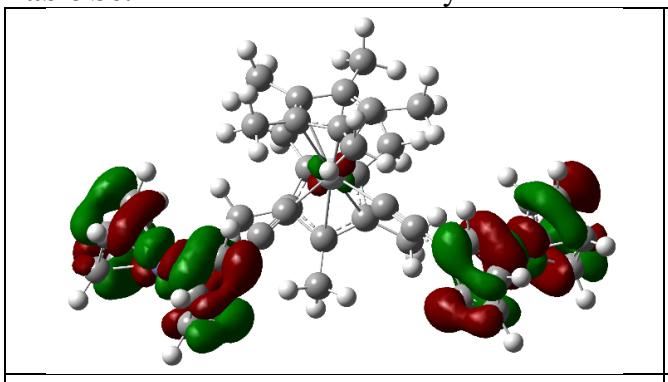	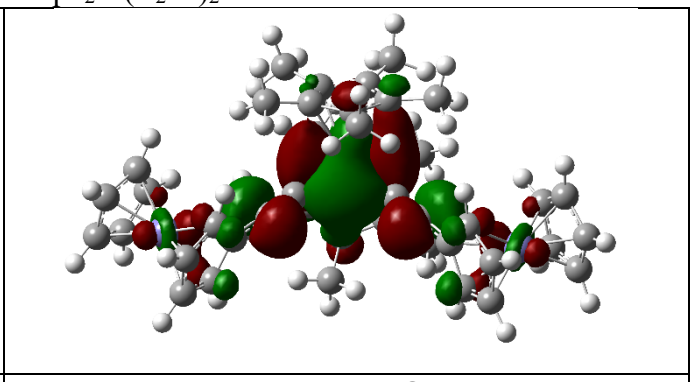
202	**194 LUMO**
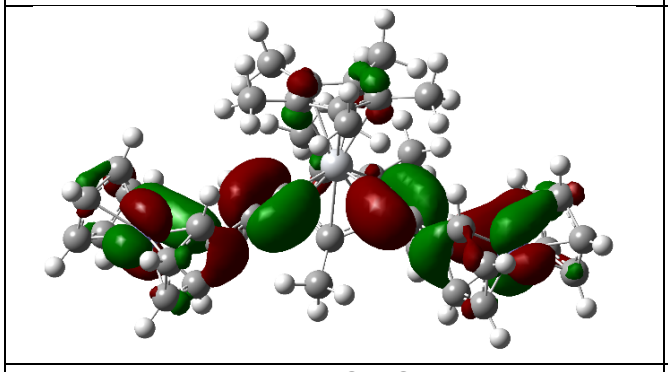	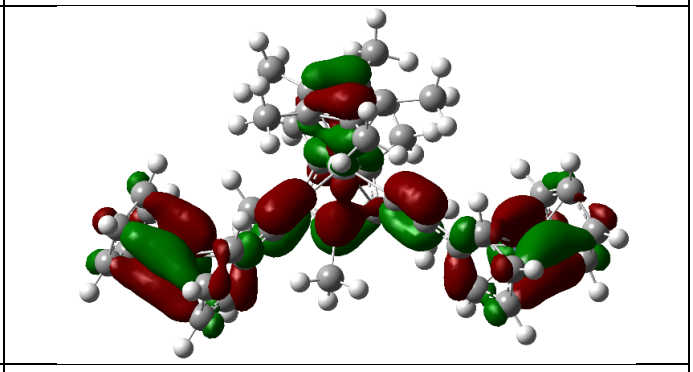
193 HOMO	**192**
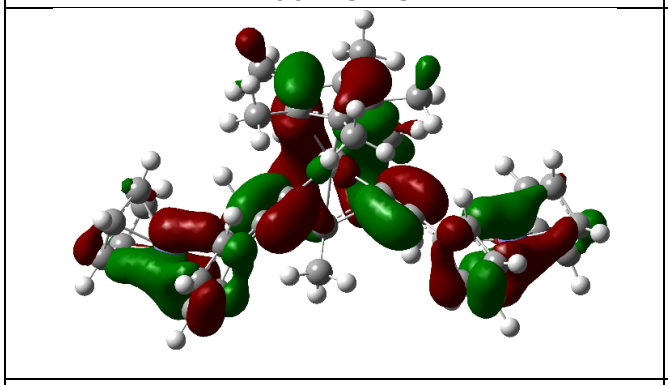	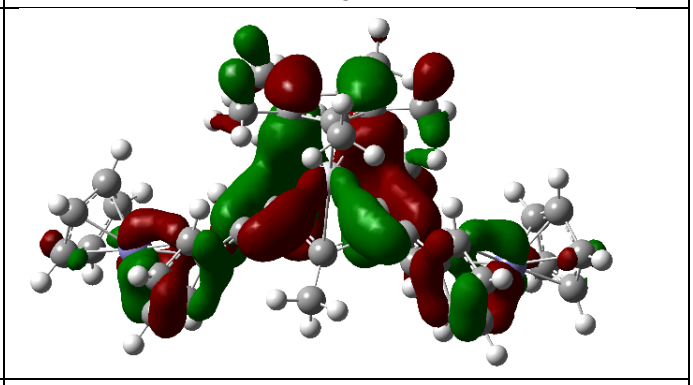
188	**186**
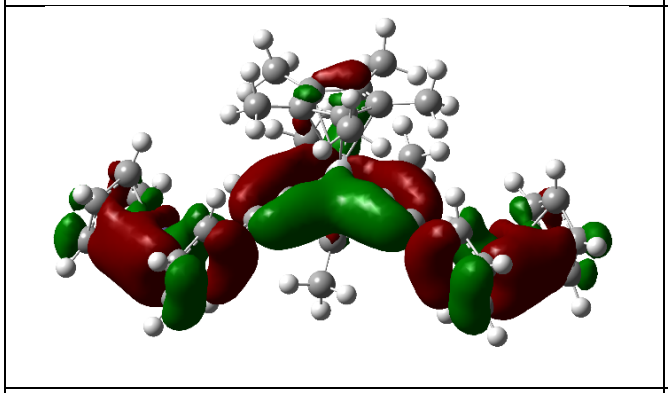	
182	

Table S7. TDDFT output for key excited states for $^{MeOOC}Cp_2Ti(C_2Fc)_2$

Excited State 1: Singlet-B 1.9940 eV 621.80 nm f=0.1767 <S**2>=0.000

181 ->184	0.20862
182 ->189	0.12784
182 ->192	-0.14716
183 ->184	***0.59217***
183 ->191	0.12769

Excited State 5: Singlet-B 2.4317 eV 509.87 nm f=0.0792 <S**2>=0.000

176 ->184	-0.12795
177 ->184	0.17243
179 ->184	***0.36707***
180 ->193	-0.25942
181 ->191	0.10204
181 ->194	-0.24097
182 ->189	0.14558
182 ->192	-0.18574
183 ->184	-0.20219
183 ->190	-0.10263
183 ->191	0.16791
183 ->194	0.10034

Excited State 15: Singlet-B 2.8211 eV 439.48 nm f=0.1081 <S**2>=0.000

175 ->193	-0.11076
176 ->184	-0.24695
176 ->194	-0.13414
177 ->184	***0.41789***
177 ->194	-0.10709
178 ->193	-0.13685
179 ->184	-0.30583
180 ->192	0.10488
180 ->193	-0.10354
181 ->184	0.14646
181 ->191	-0.12814

Excited State 20: Singlet-A 3.2990 eV 375.83 nm f=0.0629 <S**2>=0.000

174 ->184	***0.54697***
175 ->184	0.30066
182 ->185	0.20372

Table S8. Orbitals involved in key excited states for $^{MeOOC}Cp_2Ti(C_2Fc)_2$

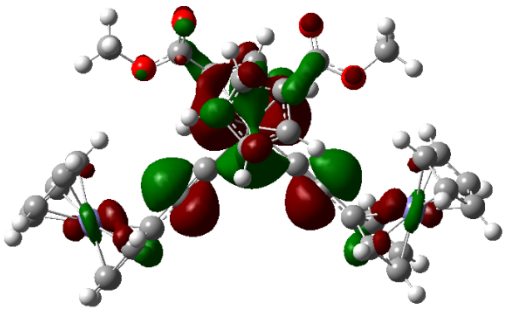	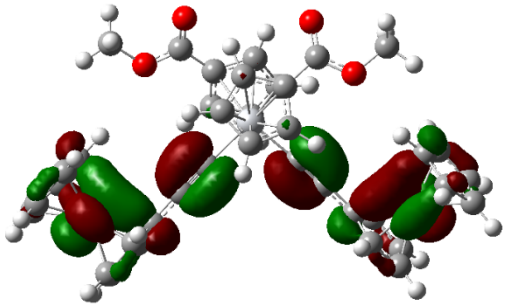
184 LUMO	183 HOMO
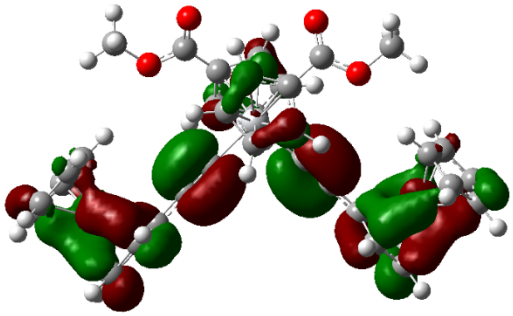	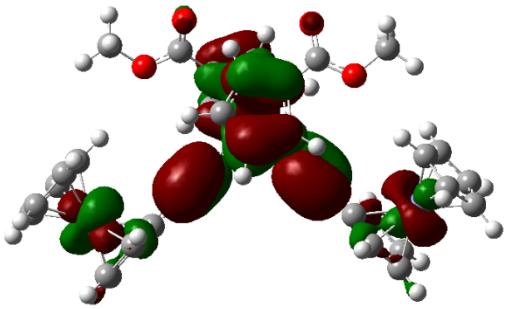
179	177
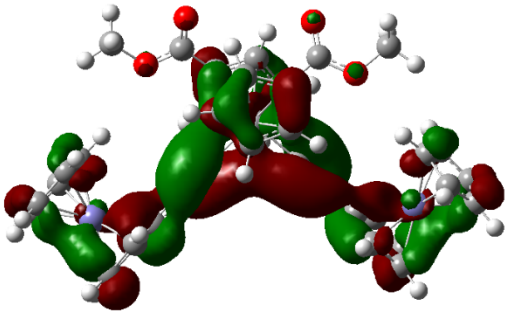	
174	

Table S9. TDDFT output for key excited states for $Cp_2Ti(C_2Fc)_2CuI$

Excited State 1: Singlet-A 2.1136 eV 586.60 nm f=0.1266 <S**2>=0.000

168 ->175	-0.10974
168 ->178	0.19668
169 ->180	0.12006
170 ->179	-0.12088
171 ->172	***0.58028***
171 ->177	0.20527

Excited State 5: Singlet-A 2.4592 eV 504.16 nm f=0.0514 <S**2>=0.000

167 ->172	**0.35043**
168 ->178	0.16426
169 ->179	-0.10802
169 ->180	0.28360
170 ->179	-0.28454
170 ->180	-0.11127
171 ->172	-0.23988
171 ->177	0.17710

Excited State 17: Singlet-A 3.0628 eV 404.81 nm f=0.1563 <S**2>=0.000

162 ->172	0.16985
164 ->172	-0.10581
165 ->172	***0.64539***

Excited State 21: Singlet-A 3.3528 eV 369.79 nm f=0.2367 <S**2>=0.000

161 ->172	***0.66693***
163 ->172	0.10231

Table S10. Orbitals involved in key excited states for $Cp_2Ti(C_2Fc)_2CuI$

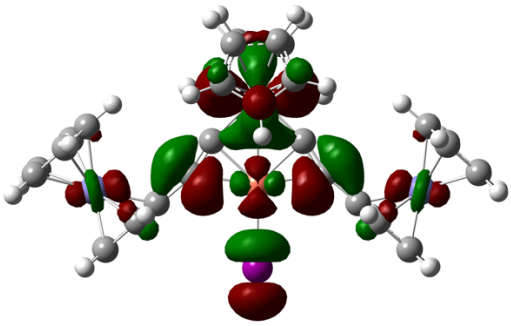	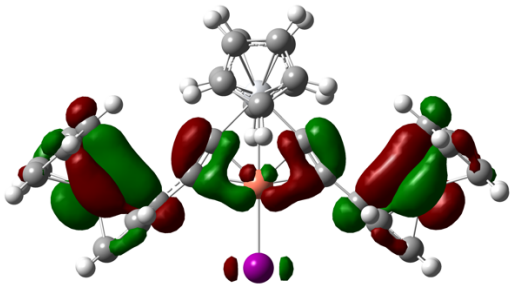
172 LUMO	171 HOMO
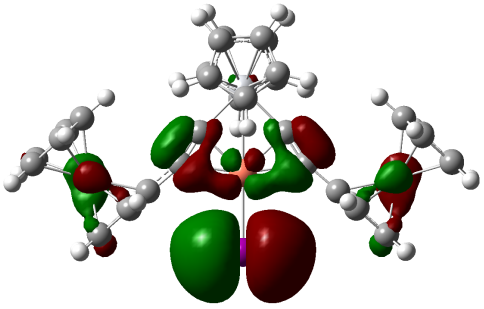	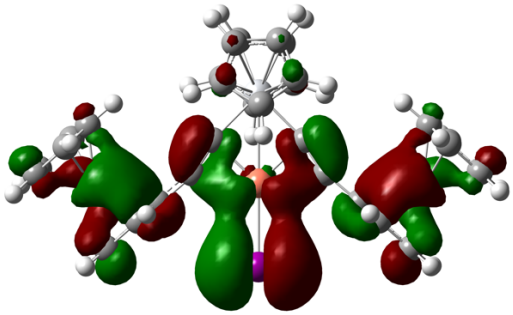
167	165
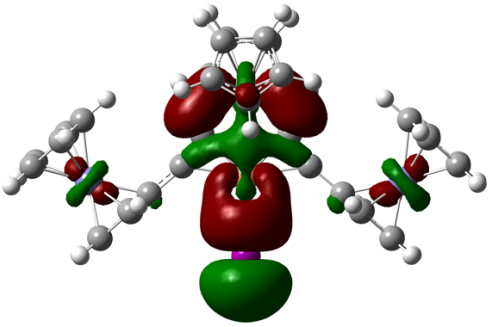	
161	